



Deposited via The University of Sheffield.

White Rose Research Online URL for this paper:

<https://eprints.whiterose.ac.uk/id/eprint/102148/>

Version: Published Version

---

**Article:**

Cassingham, N.J., Corkhill, C.L., Stennett, M.C. et al. (2016) Alteration layer formation of Ca- and Zn-oxide bearing alkali borosilicate glasses for immobilisation of UK high level waste: A vapour hydration study. *Journal of Nuclear Materials*, 479. pp. 639-646. ISSN: 0022-3115

<https://doi.org/10.1016/j.jnucmat.2016.06.009>

---

**Reuse**

Items deposited in White Rose Research Online are protected by copyright, with all rights reserved unless indicated otherwise. They may be downloaded and/or printed for private study, or other acts as permitted by national copyright laws. The publisher or other rights holders may allow further reproduction and re-use of the full text version. This is indicated by the licence information on the White Rose Research Online record for the item.

**Takedown**

If you consider content in White Rose Research Online to be in breach of UK law, please notify us by emailing [eprints@whiterose.ac.uk](mailto:eprints@whiterose.ac.uk) including the URL of the record and the reason for the withdrawal request.



Contents lists available at ScienceDirect

Journal of Nuclear Materials

journal homepage: [www.elsevier.com/locate/jnucmat](http://www.elsevier.com/locate/jnucmat)

# Alteration layer formation of Ca- and Zn-oxide bearing alkali borosilicate glasses for immobilisation of UK high level waste: A vapour hydration study

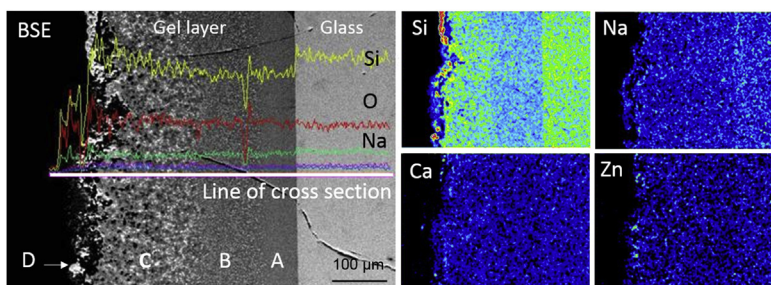
N.J. Cassingham, C.L. Corkhill\*, M.C. Stennett, R.J. Hand, N.C. Hyatt\*\*

Immobilisation Science Laboratory, Department of Materials Science and Engineering, The University of Sheffield, S1 3JD, UK

## HIGHLIGHTS

- Addition of CaO/ZnO to the UK HLW glass reduces gel layer thickness and average alteration rate.
- Hydrated Ca- and Zn-silicates are the products of CaO/ZnO modified glass alteration.
- The average alteration rate exceeds that for the French HLW simulant, SON68.

## GRAPHICAL ABSTRACT



## ARTICLE INFO

### Article history:

Received 12 February 2016

Received in revised form

31 May 2016

Accepted 2 June 2016

Available online xxx

## ABSTRACT

The UK high level nuclear waste glass modified with CaO/ZnO was investigated using the vapour phase hydration test, performed at 200 °C, with the aim of understanding the impact of the modification on the chemical composition and microstructure of the alteration layer. Experiments were undertaken on non-modified and CaO/ZnO-modified base glass, with or without 25 wt% of simulant Magnox waste calcine. The modification resulted in a dramatic reduction in gel layer thickness and also a reduction in the reaction rate, from  $3.4 \pm 0.3 \text{ g m}^{-2} \text{ d}^{-1}$  without CaO/ZnO modification to  $0.9 \pm 0.1 \text{ g m}^{-2} \text{ d}^{-1}$  with CaO/ZnO. The precipitated phase assemblage for the CaO/ZnO-modified compositions was identified as hydrated Ca- and Zn-bearing silicate phases, which were absent from the non-modified counterpart. These results are in agreement with other recent studies showing the beneficial effects of ZnO additions on glass durability.

© 2016 The Authors. Published by Elsevier B.V. This is an open access article under the CC BY-NC-ND license (<http://creativecommons.org/licenses/by-nc-nd/4.0/>).

## 1. Introduction

Understanding the long-term performance of nuclear waste glass in contact with groundwater is essential for the development

of a robust safety case for geological disposal concepts. However, because laboratory experiments are not capable of replicating the long durations expected for nuclear waste disposal ( $\sim 10^5$ – $10^6$  years), various accelerated alteration and leaching methodologies have been developed. The Vapour Phase Hydration Test (VHT) [1] provides a method of investigating the interaction between simulated nuclear waste glasses and water vapour, typically at 200 °C. At this temperature, a water film condenses on the surface of the glass specimen leading to glass hydration, ion-exchange and network

\* Corresponding author.

\*\* Corresponding author.

E-mail addresses: [c.corkhill@sheffield.ac.uk](mailto:c.corkhill@sheffield.ac.uk) (C.L. Corkhill), [n.c.hyatt@sheffield.ac.uk](mailto:n.c.hyatt@sheffield.ac.uk) (N.C. Hyatt).

<http://dx.doi.org/10.1016/j.jnucmat.2016.06.009>

0022-3115/© 2016 The Authors. Published by Elsevier B.V. This is an open access article under the CC BY-NC-ND license (<http://creativecommons.org/licenses/by-nc-nd/4.0/>).

dissolution, resulting in the rapid saturation of leached species in the film of surface water. When these species reach solution saturation concentrations, secondary phases are precipitated on the surface, which are known to play a key role in long-term glass dissolution [2], for example, in radionuclide retention or rate resumption. It has been shown that the precipitates formed under VHT conditions are similar to those formed through corrosion processes in nature [3]; assuming the overall mechanism of glass dissolution under such conditions to be comparable with that operating under representative temperatures of geological disposal, then the alteration products formed under VHT conditions may provide an insight into the possible secondary phases arising from glass dissolution under realistic conditions [4].

Here, we report preliminary results from an investigation of the vapour phase hydration of two key glass compositions from the UK high level waste vitrification programme. These are i) a Magnox waste simulant (referred to as “MW” glass), which has a nominal composition (wt%) 61.7 SiO<sub>2</sub>, 21.9 B<sub>2</sub>O<sub>3</sub>, 11.1 Na<sub>2</sub>O, 5.3 Li<sub>2</sub>O [5,6]; and ii) a modified MW glass containing CaO/ZnO, newly applied in UK HLW vitrification (referred to as MWCZ). It was recently shown that the addition of these oxides to glass creates ZnO<sub>4</sub> tetrahedra and Si-O-Zn linkages, increasing the glass network polymerisation [7,8]. As such, the addition of ZnO and CaO is reported to result in enhanced durability [9], at least during initial dissolution. Other reported benefits include reduced melt viscosity and increased levels of waste loading at lower temperatures [9,10]. During longer term dissolution, the presence of Zn has been suggested to increase the residual rate of dissolution [11,12]. In an effort to discern the nature of phases formed on the surface and in the alteration layer of these glasses, and the role of CaO and ZnO additions to Magnox waste glass, the vapour phase hydration of MW and MWCZ glass specimens was studied for periods of 10–30 days in saturated water vapour. The progress of alteration was evaluated by analysis of the alteration layer thickness by Scanning Electron Microscopy (SEM), and the chemical nature of the hydration layer and alteration products was performed using Energy Dispersive X-ray (EDX) and X-ray Diffraction (XRD) analysis.

## 2. Experimental methodology

Base glass compositions of MW and MWCZ glasses were prepared using glass frits supplied by National Nuclear Laboratory (NNL). In addition to the base glasses, two further samples were prepared, which were blended with 25 wt% simulant Magnox waste oxides; these glasses are referred to as MW-25 and MWCZ-25. The addition of simulant waste oxides was performed by adding a calcine, also supplied by NNL (MW-25), or by raw components supplied by Alfa Aesar with >99.0% purity (MWCZ-25). Mixed glass batches were added to a mullite crucible and placed in an electric furnace at 1060 °C for 1 h, and subsequently stirred for 3 h at temperature. The glasses were cast into a pre-heated stainless steel mould and the resulting blocks were annealed at 500 °C for 1 h and cooled to room temperature at 1 °C min<sup>-1</sup>. The x-ray Fluorescence spectroscopy (Panalytical) analysed compositions of the final glasses are given in Table 1.

A diamond slow saw was applied to cut monoliths of 10 mm × 10 mm × 1.5 mm (± 0.1 mm), which were polished to a finish of 600 grit, on all sides. The polished monoliths were cleaned ultrasonically for 2 min in ethanol and dried overnight at 110 °C. Density measurements were performed on each monolith using the Archimedes method with ethanol solute. Vapour Hydration Test experiments were performed according to Jiricka et al. [1] and ASTM method C1663-09 [13]. Briefly, two coupons of glass were suspended in Parr series 4700 pressure vessels (22 cm<sup>3</sup> volume) using support frames and Type 304 stainless steel wires. At the

**Table 1**

Analysed compositions (wt%) of the base and waste simulant-blended glasses used in VHT experiments.

Oxide component	MW	MW-25	CZMW	CZMW-25
SiO <sub>2</sub>	60.27	46.28	56.1	46.44
B <sub>2</sub> O <sub>3</sub>	24.11	18.30	21.51	18.95
Na <sub>2</sub> O	10.88	8.12	11.48	9.32
Li <sub>2</sub> O	4.75	4.81	2.92	2.27
CaO	–	–	1.94	1.54
ZnO	–	–	6.03	4.28
Al <sub>2</sub> O <sub>3</sub>	–	1.87	–	0.11
BaO	–	1.22	–	1.67
CeO <sub>2</sub>	–	1.24	–	1.28
Cr <sub>2</sub> O <sub>3</sub>	–	0.37	–	0.19
Cs <sub>2</sub> O	–	1.61	–	1.42
Fe <sub>2</sub> O <sub>3</sub>	–	1.87	–	0.49
Gd <sub>2</sub> O <sub>3</sub>	–	3.86	–	2.62
La <sub>2</sub> O <sub>3</sub>	–	0.67	–	0.71
MgO	–	1.34	–	0.11
MoO <sub>3</sub>	–	2.02	–	2.41
Nd <sub>2</sub> O <sub>3</sub>	–	1.81	–	1.69
NiO	–	0.28	–	0.18
Pr <sub>2</sub> O <sub>3</sub>	–	0.47	–	0.46
RuO <sub>2</sub>	–	0.49	–	0.46
Sm <sub>2</sub> O <sub>3</sub>	–	0.28	–	0.28
SrO	–	0.32	–	0.43
TeO <sub>2</sub>	–	0.28	–	0.12
Y <sub>2</sub> O <sub>3</sub>	–	0.1	–	0.11
ZrO <sub>2</sub>	–	2.4	–	2.48
Total	100	100	100	100
Density (g cm <sup>-3</sup> ) ± 0.02	2.77	2.81	2.61	2.65

reaction temperature, it was determined that 200 µL of ultra-high quality water (18.2 MΩ cm at 25 °C) was sufficient to provide a non-dripping surface layer of water on the coupons. The pressure vessels were tightly sealed and placed in an oven at 200 °C ± 1 °C for 10–30 days. At the end of each experiment, vessels removed from the oven were quenched in a bath of cold water. No evidence of dripping of water from the coupons was apparent in any of the experiments, as determined by the approximately neutral pH of the condensed water vapour at the end of the experiment. Coupons of glass were mounted in epoxy resin and polished to a finish of 1 µm with diamond paste for SEM/EDX analysis using a JEOL 6400 SEM equipped with an Oxford Link EDX system and a Hitachi TM3030 SEM equipment with a Bruker Quantax 70 EDX system. X-ray diffraction of unmounted samples were acquired using a Siemens D5000 X-ray Powder Diffractometer with Cu Kα radiation, from 5 to 90° 2θ with a step size of 0.02 at 0.1° min<sup>-1</sup>.

## 3. Results

Examination of the simulant UK HLW glasses using back scattered electron microscopy (Fig. 1) after 10, 20 and 30 days of exposure to the VHT experimental conditions revealed the presence of a gel layer, ranging in thickness from 1 to 475 µm in size. Table 2 and Fig. 2 summarise the thickness of the layer at each time point and the rate of alteration; the gel layer was observed to increase in thickness with reaction time. The average alteration rate (g m<sup>-2</sup> d<sup>-1</sup>) was approximated from the measured gel rate in µm d<sup>-1</sup>, multiplied by the glass density (in g cm<sup>-3</sup>), following Neeway et al. [16], as shown in Equation (1). This approach assumes a constant rate of reaction; Fig. 2 shows that within error, this is a reasonable assumption to make for all glasses investigated.

$$R = \rho \frac{\Delta g}{\Delta t} \quad (1)$$

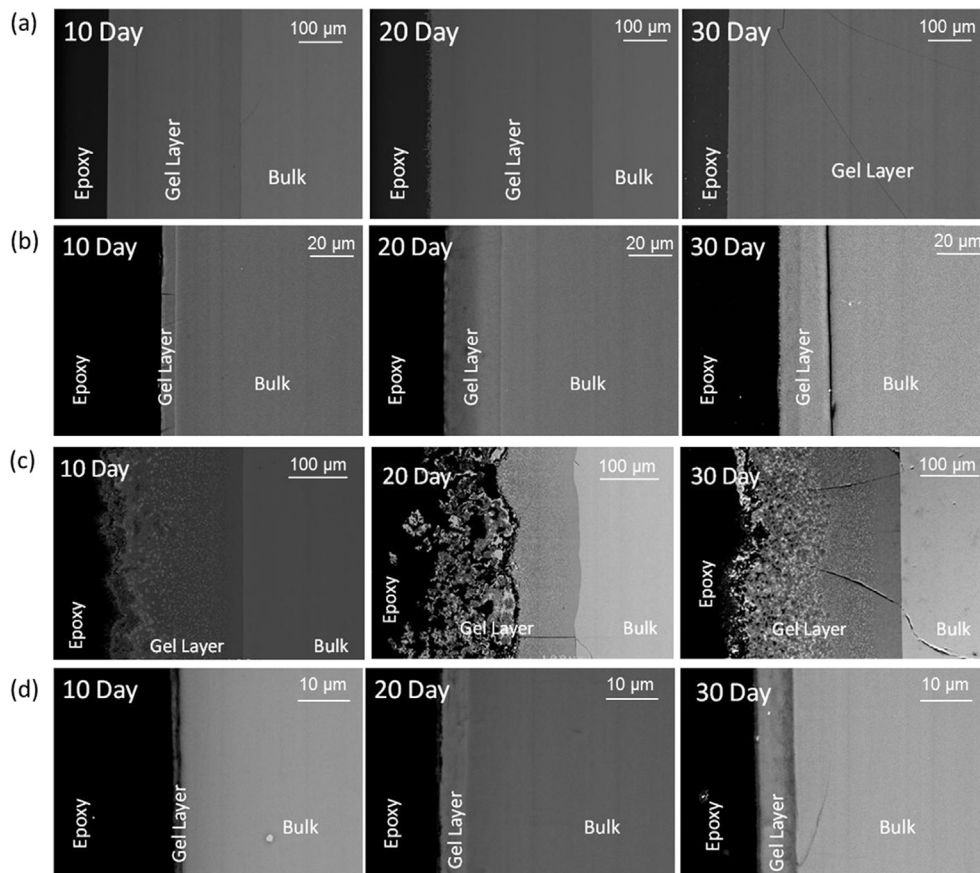


**Fig. 1.** Back-scattered electron image of the cross section obtained from coupons of (a) MW base glass; (b) MW-25; (c) MWCZ base glass and; (d) MWCZ-25, subject to vapour phase hydration conditions at 200 °C for 10, 20 and 30 days. NB: different magnifications for each sample.

**Table 2**

Thickness of the gel layer of each glass sample subject to VHT conditions (200 °C) for 10–30 days, rate of gel layer formation (according to Fig. 2), calculated alteration rate and phases identified by XRD, as shown in Fig. 3. The estimated error on all gel layer thickness measurements in this investigation is  $\pm 10\%$ .

	Gel layer thickness ( $\mu\text{m}$ )			Gel layer growth rate ( $\mu\text{m d}^{-1}$ )	Alteration rate ( $\text{g m}^{-2} \text{d}^{-1}$ )	Phases identified by XRD
	10 d	20 d	30 d			
<i>This work</i>						
MW	296	368	475	$8.95 \pm 0.9$	$24.8 \pm 2.5$	$\text{SiO}_2$ (quartz), $\text{Na}(\text{AlSi}_2\text{O}_6) \cdot (\text{H}_2\text{O})$ (analcime)
MW-25	7	25	31	$1.20 \pm 0.1$	$3.4 \pm 0.3$	$\text{SiO}_2$ (quartz), $\text{Na}_{0.61}\text{Al}_{4.70}\text{Si}_{7.32}\text{O}_{20}(\text{OH})_4$ , $\text{Na}_3\text{Al}_3\text{Si}_3\text{O}_{12} \cdot 2\text{H}_2\text{O}$ (fabriesite)
MWCZ	250	275	325	$3.75 \pm 0.4$	$9.8 \pm 1.0$	$\text{SiO}_2$ (quartz), $\text{Ca}_2\text{SiO}_4 \cdot \text{H}_2\text{O}$ , $\text{Zn}_2\text{SiO}_4 \cdot \text{H}_2\text{O}$ (hemimorphite)
MWCZ-25	1	6	8	$0.35 \pm 0.1$	$0.9 \pm 0.1$	$\text{Ca}_2\text{SiO}_4 \cdot \text{H}_2\text{O}$ , $\text{Zn}_2\text{SiO}_4 \cdot \text{H}_2\text{O}$ (hemimorphite), $\text{SiO}_2$ (quartz), $\text{ZrSiO}_4$ (zircon)
<i>Literature*</i>						
MW-25 [14] <sup>a</sup>	4.6	5.2	6.2	0.12	0.3	$(\text{Na},\text{M})_x(\text{Si},\text{Al},\text{A},\text{M})_4\text{O}_{10}(\text{OH})_2 \cdot 4\text{H}_2\text{O}$ (M, metal; A, lanthanide or Ca); $(\text{Ca},\text{Sr},\text{Ba})\text{MoO}_4$ ; Zr-silicate
MWCZ-20 [7] <sup>b</sup>	–	–	10	–	–	Ca,Si,Na containing phases
SON68 [15] <sup>c</sup>	–	0.5	–	0.03	0.07	$\text{NaAlSi}_2\text{O}_6 \cdot \text{H}_2\text{O}$ ; $\text{Ca}_5\text{Si}_6\text{O}_{16}(\text{OH})_2 \cdot n\text{H}_2\text{O}$ ; $\text{Ca}_5(\text{PO}_4)_2(\text{OH})$ ; $\text{Na}_2\text{SiO}_3 \cdot 5\text{H}_2\text{O}$ ; $(\text{Ca},\text{Sr})\text{Mo}_3\text{O}_9(\text{OH})_2$
SON68 [16] <sup>d</sup>	–	–	–	4.00	0.19	$\text{Ca}_5\text{Si}_6\text{O}_{16}(\text{OH})_2 \cdot n\text{H}_2\text{O}$ ; $\text{CaMoO}_4$ ; $\text{NaAlSi}_2\text{O}_6 \cdot \text{H}_2\text{O}$ ; $\text{CaCO}_3$

\* VHT experiments were nominally identical and performed for a duration of: <sup>a,b</sup> 28 days; and <sup>c</sup> 1000 days. <sup>d</sup> VHT experiments were performed for 57 days, under excess water conditions.

Where R is the alteration rate ( $\text{g m}^{-2} \text{d}^{-1}$ ),  $\rho$  the glass density ( $\text{g cm}^{-3}$ ) (Table 1),  $\Delta g$  the change in gel layer thickness between 10 and 30 days, and  $\Delta t$  the change in time between 10 and 30 days.

The rate of gel layer growth and overall morphology was highly dependent on the glass composition. On the outer edge of the gel layer (i.e., between the gel layer and the epoxy), a layer of precipitates of varying thickness was observed. Analysis of the surface of the glass coupon, performed by X-ray diffraction (XRD),

confirmed the presence of crystalline phases (Fig. 3), the composition of which were dependent on the glass composition. A detailed description of the morphology and chemical nature of each glass gel layer and the precipitated phases is given below.

### 3.1. MW base glass

The gel layer of the MW base glass developed at a rate of

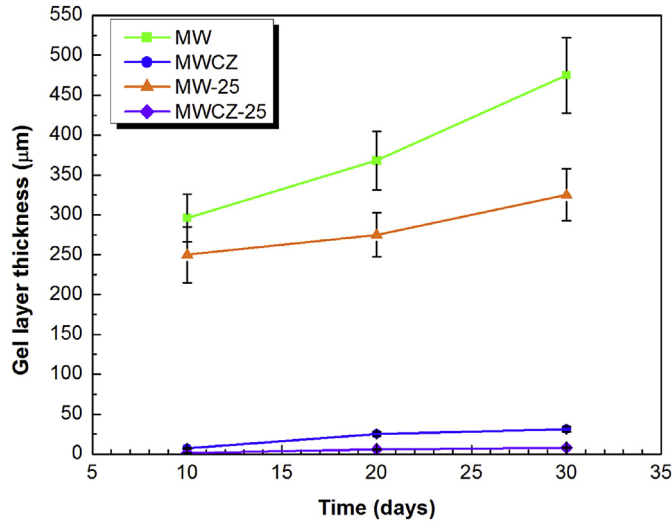


**Fig. 2.** Gel layer thickness as a function of time for MW base glass; MW-25; MWCZ base glass and; MWGZ-25, subject to vapour phase hydration conditions at 200 °C for 30 days. The estimated error on all gel layer thickness measurements in this investigation is  $\pm 10\%$ .

$8.95 \pm 0.9 \mu\text{m d}^{-1}$ , giving a final thickness at 30 days of  $475 \pm 47.5 \mu\text{m}$  (Fig. 1a and 2; Table 2). This corresponds to an alteration rate of  $24.8 \pm 2.5 \text{ g m}^{-2} \text{ d}^{-1}$ . Energy dispersive X-ray (EDX) line scan analysis of this region at 30 days was performed to determine the distribution of key glass matrix elements (Si, Na, O) (Fig. 4). The gel layer was characterised by elevated O and depleted Si and Na concentrations, relative to the bulk glass (Zone A, Fig. 3). There was a small enhancement in the concentration of Si towards the outer edge of the gel layer.

A thin layer of crystalline precipitates was identified on the surface of the gel layer; back-scattered electron and EDX analysis of this region (Fig. 4, ROI) revealed acicular crystallites,  $15 \pm 1.5 \mu\text{m}$  in length. EDX mapping of these precipitates demonstrated a lower Si, but similar O and Na, concentrations compared to the gel layer. X-ray diffraction analysis was performed on the surface of the glass coupon at 0, 10, 20 and 30 days of reaction (Fig. 3a). Prior to the VHT experiment, two regions of diffuse scattering were observed between  $15$  and  $35^\circ 2\theta$  and  $40$ – $55^\circ 2\theta$ , highlighting the amorphous nature of the glass. After 10 days, only diffuse scattering was apparent, suggesting that the gel layer ( $296 \pm 30 \mu\text{m}$  in thickness) was also amorphous, confirmed by the absence of precipitates in Fig. 1a. At 20 and 30 days of exposure to the VHT conditions, diffraction peaks indexed to quartz ( $\text{SiO}_2$ , [PDF 04-0379]) and the sodium aluminium silicate phase, analcime ( $\text{Na}(\text{AlSi}_2\text{O}_6) (\text{H}_2\text{O})$ , [PDF 70-1575]) were observed on top of the region of diffuse scattering between  $15$  and  $35^\circ 2\theta$ . The identification of these phases is in agreement with the presence of Si, O and Na in the EDX map analysis (Fig. 4).

### 3.2. MW-25 glass

A thin gel layer, which formed at a rate of  $1.2 \pm 0.1 \mu\text{m d}^{-1}$  ( $3.4 \pm 0.3 \text{ g m}^{-2} \text{ d}^{-1}$ ) with a total thickness of  $31 \pm 3 \mu\text{m}$  after 30 days was observed in back-scattered electron analysis of the MW-25 cross sections (Figs. 1b, 2 and 5). This layer was separated from the glass by a region with dark contrast (Fig. 5), which is attributed to shrinkage of the gel layer during drying. At the interface between the glass and the drying “gap” there was an elevated concentration of Si, O and Na; in their recent analysis of borosilicate glass dissolution, Geisler et al. [17] observed similar local enrichment, which they attributed to inefficient transport of elements from the glass as the thickness of the gel layer increases.

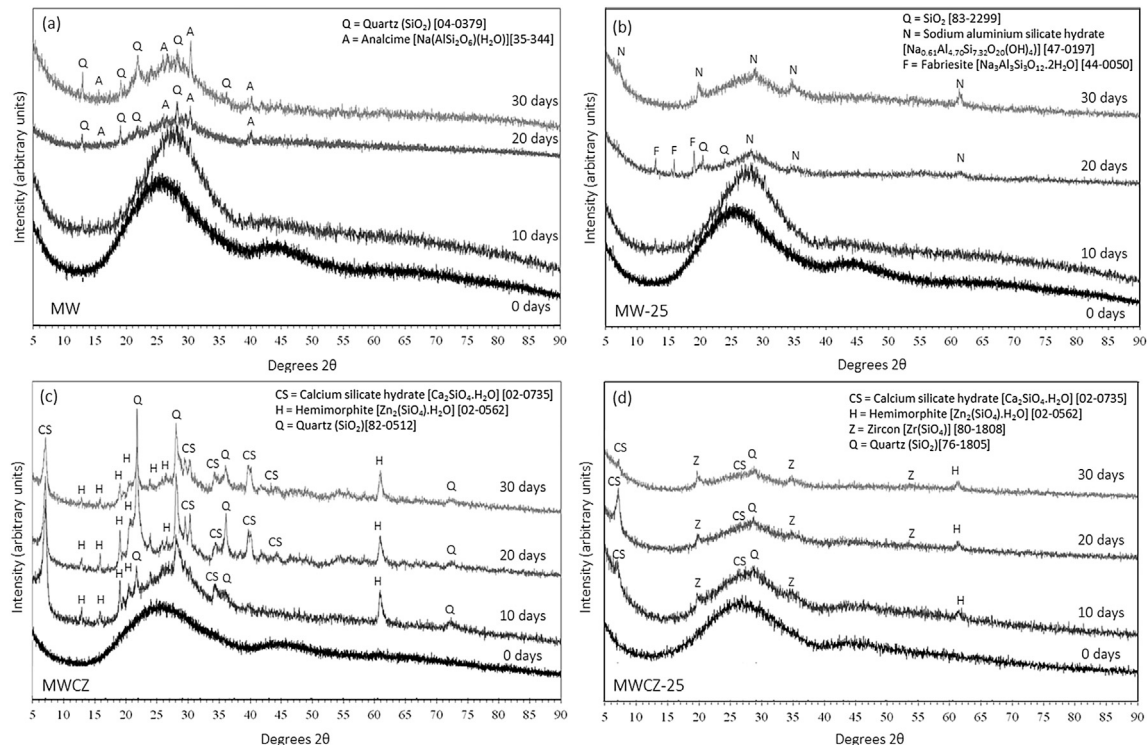


**Fig. 3.** X-ray diffraction patterns of (a) MW base glass; (b) MW-25; (c) MWCZ base glass and; (d) MWCZ-25, subject to vapour phase hydration conditions at 200 °C for 10, 20 and 30 days. Diffraction patterns for non-leached glass coupons are also shown for comparison (0 days).

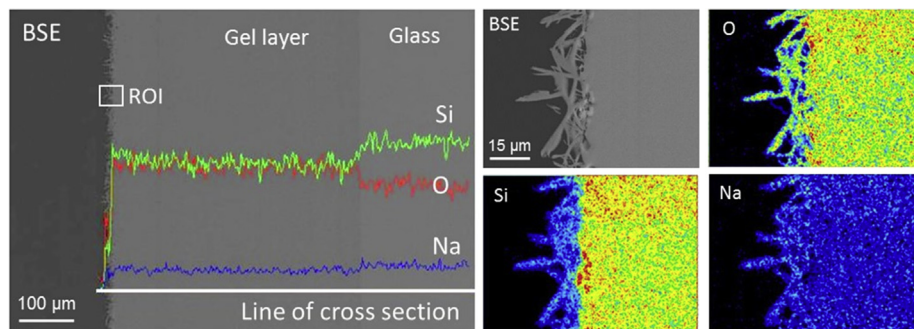


**Fig. 4.** Back-scattered electron image of the cross section obtained from a coupon of MW base glass subject to vapour phase hydration conditions at 200 °C for 30 days. Profile of selected elements across the gel and precipitate layers are shown and zones of different contrast, Zone A and Zone B. A region of interest (ROI) at the surface was further investigated for elemental content using EDX.

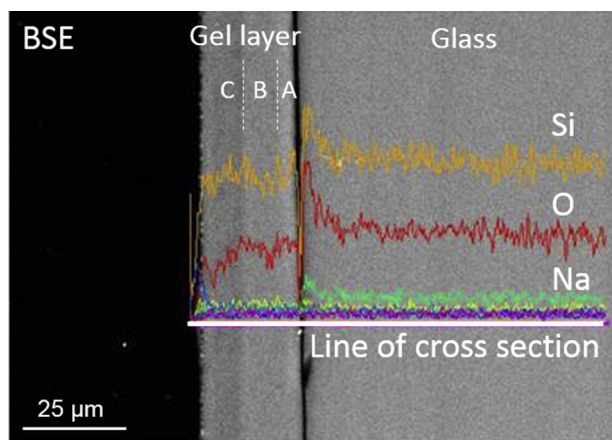


**Fig. 5.** Back-scattered electron image of the cross section obtained from a coupon of MW-25 glass subject to vapour phase hydration conditions at 200 °C for 30 days. The profile of selected elements across the gel layer, as analysed by EDX, are shown.

Detailed examination of the gel layer revealed three regions; the first and brightest region (Zone A) was approximately 6 µm in thickness and characterised by a steep gradient in Si, whereas the concentration of Na and O was invariant (Fig. 5). The middle region (Zone B) was ~9 µm in thickness and had variable O and Si content. At the interface between Zones B and C (~10 µm thick) there was an increase in the concentrations of both Si and O, which also occurred at the outer edge of Zone C. Crystalline precipitates were also observed on the outer region of the gel layer (Figs. 1b and 5); XRD analysis revealed the presence of two hydrated sodium aluminosilicate phases, the clay-like  $\text{Na}_{0.61}\text{Al}_{4.70}\text{Si}_{7.32}\text{O}_{20}(\text{OH})_4$  [PDF 47-0197] and fabriesite,  $\text{Na}_3\text{Al}_3\text{Si}_3\text{O}_{12} \cdot 2\text{H}_2\text{O}$  [PDF 44-0050]), in addition to quartz ( $\text{SiO}_2$ , [PDF 83-2299]). This latter phase was observed only in the 20 day sample, suggesting that it was heterogeneously distributed throughout the precipitate layer, hence not always sampled by XRD. The most significant contribution to all XRD patterns was the diffuse scattering peaks at 15 and 35° 2θ and 40–55° 2θ, indicating the largely amorphous nature of the alteration layer (Fig. 3b).

### 3.3. MWCZ base glass

Back-scattered electron analysis of cross sections of the MWCZ base glass, shown in Figs. 1c and 6, revealed the formation of a complex gel layer, which formed at a rate of  $3.75 \pm 0.4 \mu\text{m d}^{-1}$ , giving a final thickness at 30 days of  $325 \pm 33 \mu\text{m}$ . This corresponds to an alteration rate of  $9.8 \pm 1.0 \text{ g m}^{-2} \text{ d}^{-1}$ . The gel layer at 30 days

comprised four distinct regions (Zones A – D, Fig. 5), identified by changes in contrast, texture and elemental composition. Zone A was slightly depleted in Si and Na with respect to the bulk glass and was ~70 µm in thickness. At the interface of Zones A and B, there was a sharp decrease in Si, O and Na content. Zone B (~100 µm thick) was characterised by a significant change in morphology; this layer appeared to be more porous than Zone A, and concentration of profiles of Si, O and Na were similar to those in Zone A. Zone C, corresponding to the ~190 µm thick band of brighter contrast in the back-scattered electron image shown in Fig. 5, was characterised by a concentration gradient of Si and Ca (increasing towards the outer gel layer surface) and a greater porosity than exhibited in Zone B. The outer surface of the alteration layer, Zone D, showed enhanced concentrations of Si, O, Zn and Ca (Fig. 6).

X-ray diffraction analysis of MWCZ base glass is shown in Fig. 3c. Prior to the VHT experiment, and after 10 days of reaction, the diffraction patterns showed two regions of broad diffuse scattering between 15 and 40° 2θ and 40–50° 2θ. The 10 day sample exhibited additional diffraction peaks, which were indexed to calcium silicate hydrate ( $\text{Ca}_2\text{SiO}_4 \cdot \text{H}_2\text{O}$  [PDF 02-0735]), the hydrated Zn-silicate, hemimorphite ( $\text{Zn}_2\text{SiO}_4 \cdot \text{H}_2\text{O}$  [PDF 02-0562]), and quartz ( $\text{SiO}_2$  [PDF 82-0512]). After 20 days of VHT reaction, the region of diffuse scattering decreased in relative intensity, while the intensity of diffraction peaks of the other phases increased, highlighting the increasing formation of crystalline phases as a function of dissolution. These phases were also present after 30 days of reaction and correspond to the high Si, Zn and Ca concentrations observed in the EDX maps of Zone D (Fig. 6).

### 3.4. MWCZ-25 glass

In contrast to the MWCZ base glass, MWCZ-25 glass exhibited a thin gel layer (Fig. 1d) that developed at a rate of  $0.35 \pm 0.01 \mu\text{m d}^{-1}$ , equivalent to an alteration rate  $0.9 \pm 0.1 \text{ g m}^{-2} \text{ d}^{-1}$  (Table 2, Fig. 2). After 30 days of VHT reaction, the layer was  $8 \pm 0.8 \mu\text{m}$  in thickness and was found to be pulled away from the glass (due to dehydration during drying and analysis) (Fig. 7), leaving a gap in the EDX analysis; hence elucidation of different zones within this layer was not straightforward. Nevertheless, it was possible to characterise the gel layer with having slightly lower Si, O and Na concentrations than the bulk glass, but similar concentrations of Ca, Zn, Mg and Zr. The precipitate layer comprised a very thin band (<1 µm) of crystallites, which were confirmed as calcium silicate hydrate ( $\text{Ca}_2\text{SiO}_4 \cdot \text{H}_2\text{O}$  [PDF 02-0735]) and, tentatively, zircon ( $\text{ZrSiO}_4$ , [PDF 80-1808]) and hemimorphite ( $\text{Zn}_2\text{SiO}_4 \cdot \text{H}_2\text{O}$  [PDF 02-0562]) by XRD. All phases were apparent in the diffraction data after just 10 days of reaction (Fig. 3d). The diffuse scattering peaks at 15 and 40° 2θ and 40–50° 2θ were the dominant feature of the XRD patterns;

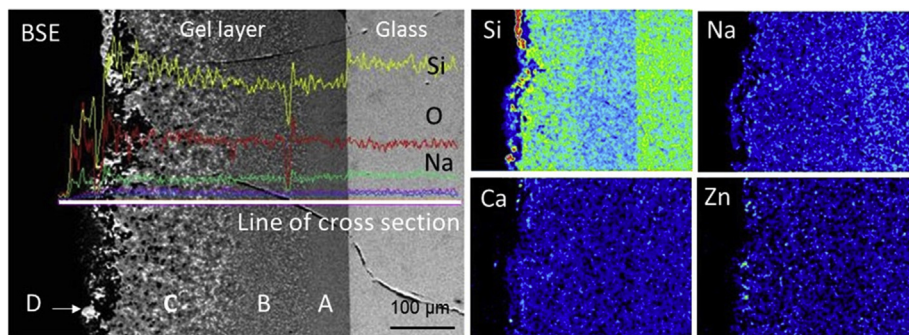


**Fig. 6.** Back-scattered electron image, EDX elemental line scans and EDX mapping of key elements of MWCZ base glass subjected to vapour phase hydration conditions at 200 °C for 30 days.

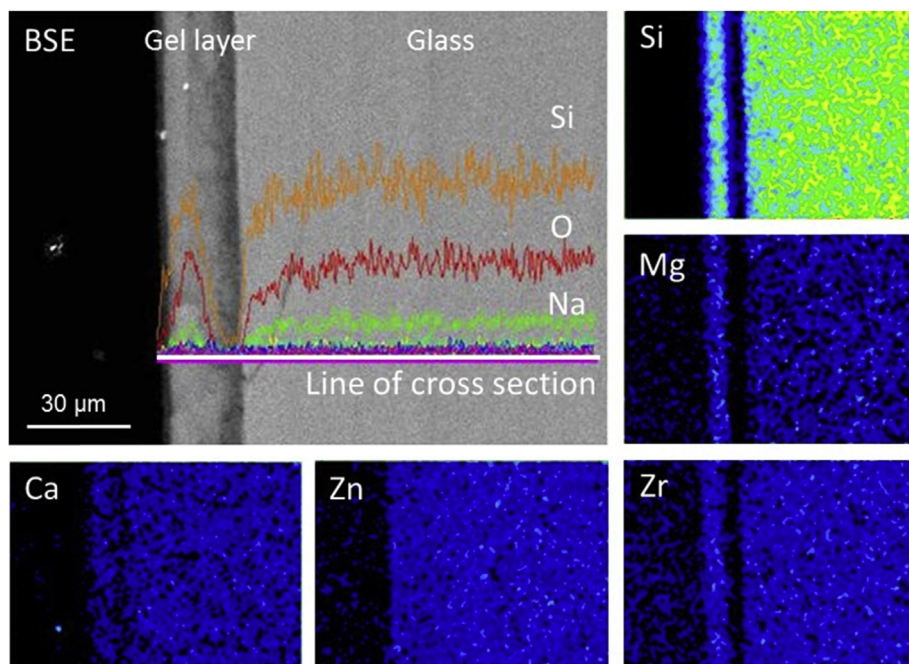


**Fig. 7.** Back-scattered electron image, EDX elemental line scans and EDX mapping of key elements of MWCZ-25 glass subjected to vapour phase hydration conditions at 200 °C for 30 days.

due to the very thin nature of the crystalline precipitate layer, the XRD sampling incorporated a significant volume of the underlying amorphous gel layer.

## 4. Discussion

### 4.1. Non-modified MW glass compositions

The vapour phase hydration of MW glass resulted in the formation of a thick, generally amorphous gel layer, with quartz and (Al, Na)-silicate (analcime) crystalline products. The addition of 25 wt% waste simulant to the base glass significantly decreased the rate of alteration; the gel layer thickness was a factor of 15 lower than the non-waste loaded counterpart. This is in agreement with previous studies of this glass composition, which showed that increasing the waste loading of MW base glass enhances durability, up to 38 wt% [18]; enhanced durability of waste loaded glasses is due to an increased concentration of network formers (e.g. Zr, Si, Ln) compared with non-waste loaded counterparts.

The final thickness of the gel layer of MW-25 at 30 days

( $31 \pm 0.3 \mu\text{m}$ ) was significantly greater than that observed by Hyatt et al. [14] under nominally identical VHT conditions, which gave an alteration layer of  $6.2 \mu\text{m}$ , however the glass composition varied slightly between these two studies; the MW-25 utilised by Hyatt et al. incorporated a Magnox waste simulant blended with oxide simulant waste from the ThORP process, while the composition investigated herein comprised Magnox waste simulant only. Subtle differences in composition of these glasses are observed in the B and Li content; B and Li are notably higher in the glass investigated in the current paper, at 17.8 mol%  $\text{B}_2\text{O}_3$  giving a  $\text{SiO}_2:\text{B}_2\text{O}_3$  ratio of 2.9, compared with 16.0 mol% in the study of Hyatt et al., giving a  $\text{SiO}_2:\text{B}_2\text{O}_3$  ratio of 3.3. Similarly,  $\text{Li}_2\text{O}$  was 10.9 % in this work, compared with 9.1 mol% for Hyatt et al. It was recently shown that borosilicate glasses with a high Li content are a combination of Li-silicate and borate networks, while those with a lower Li content use Li to charge compensate for  $\text{BO}_4$  units in the borosilicate network [19]. In glass dissolution theory, alkali ions, such as Na and Li, are the first to be leached from the glass, which results in hydrolysis and breakdown of the silicate glass network; therefore, the higher alkali content in the current investigation compared with

that of Hyatt et al. [14] may be the origin of the enhanced gel layer thickness. In accordance with a greater gel layer thickness in the current study, the alteration rate was also greater than observed by Hyatt et al., at  $3.7 \pm 0.04 \text{ g m}^{-2} \text{ d}^{-1}$  compared with  $0.3 \pm 0.04 \text{ g m}^{-2} \text{ d}^{-1}$  [14] (Table 2).

The results presented here are in agreement with previous observations that MW-25 is less durable than the French high level nuclear waste simulant glass, SON68 [5]. For example Gong et al. [15] reported a SON68 alteration layer thickness of  $0.5 \mu\text{m}$  after 22 days, under similar VHT conditions, while Neeway et al. [16] reported an alteration layer thickness of  $4 \mu\text{m}$  after 57 days (Table 2). In accordance with this observation, the alteration rate of MW-25 was also found to be higher than that of SON68, with values of  $3.7 \pm 0.04 \text{ g m}^{-2} \text{ d}^{-1}$  for MW25 and  $0.07 \text{ g m}^{-2} \text{ d}^{-1}$  for SON68 [15]. The SON68 alteration rate derived from the work of Neeway et al. is also lower than that observed for MW-25 in the current study ( $0.19 \text{ g m}^{-2} \text{ d}^{-1}$ ), however, the VHT conditions of these studies are not directly comparable; Neeway et al. deviated from the ASTM standard [13] by using a relative humidity of 92% (compared with 100% in the present study) and by using a large volume of water in the reaction vessel [16], which significantly enhances the alteration rate. Nevertheless, the alteration rates observed for MW-25 and SON68 are up to 1.5 times lower than the observed forward rate [15,16,20]. The variation in durability between MW-25 and SON68 may be due to differences in the B and Li content of these glasses (14.1 mol%  $\text{B}_2\text{O}_3$  for SON68, compared with 17.8 mol% in the present study, and 4.6 mol%  $\text{Li}_2\text{O}$  for SON68, compared with 10.9 mol% for MW-25) as discussed above. However, it has also been postulated that Mg, which is absent from SON68, plays a role in enhancing the dissolution of MW-25 compared with SON68 [5]. The presence of CaO and ZnO in SON68 is also reported to confer enhanced durability in the initial stages of dissolution [9,10].

The precipitated products identified on the surface of the MW glass compositions were a (Na, Al)-containing silicate and clay, and quartz. This differs from the reaction products found in liquid-based dissolution experiments of the same glass, where Mg-bearing clay precipitates, such as montmorillonite [5] and sepiolite [6] were identified, but is comparable to Hyatt et al. who identified the presence of Na, Al-smectite clay in their VHT analysis of MW-25 [14]. In agreement with previous observations on the French R7T7 glass [21], this indicates that although the VHT conditions are capable of replicating dissolution rate trends observed in liquid water experiments, they are not able to fully represent the phases formed during long-term dissolution at temperatures  $< 200 \text{ }^\circ\text{C}$ .

#### 4.2. CaO/ZnO - modified MW glass compositions

The addition of oxides of Ca and Zn to the MW base glass composition resulted in the formation of a gel layer with variable porosity, which was characterised by the formation of quartz, and hydrated Ca- and Zn-bearing silicate phases (hydrated calcium silicate and hemimorphite, Table 2). The gel layer of the CaO/ZnO base glass was more than 3 times smaller than the MW base glass after 30 days (at  $8.0 \pm 0.8 \mu\text{m}$  and  $0.35 \pm 0.04 \mu\text{m}$ , respectively). With the addition of 25 wt% waste simulant, the rate of alteration was reduced further still, to  $0.9 \pm 0.1 \text{ g m}^{-2} \text{ d}^{-1}$ . The rate derived from this investigation differs somewhat with that of Zhang et al. [7] who reported the dissolution of the same glass, albeit with 20 wt% of simulant waste oxides (i.e. MWCZ-20), giving a rate of  $\text{NL}_B = 0.107 \pm 0.003 \text{ g m}^{-2} \text{ d}^{-1}$  for liquid water experiments at  $90 \text{ }^\circ\text{C}$  with a surface area to volume ratio of  $1200 \text{ m}^{-1}$ . The variation in rate derived from these different experimental methods is not unexpected; the corrosion mechanism in the vapour phase is influenced by a high ratio of glass to water vapour, leading to a

higher pH and, therefore, a higher alteration rate than in liquid water. The same authors also investigated the dissolution of MWCZ-20 under VHT conditions, and reported a comparably thick gel layer after 28 days ( $\sim 10 \mu\text{m}$ , compared with  $8 \pm 0.8 \mu\text{m}$  in the present study), composed of Si and minor Al, with precipitates containing Ca, Si and Na [7]. The precipitated phases in the present study of MWCZ-25 were found to be similar to that of the CZMW base glass, comprising quartz, hydrated Ca- and Zn-silicates, in addition to zircon ( $\text{ZrSiO}_4$ ), which is tentatively assigned from weak reflections in the XRD data (Fig. 3d).

The gel layer thickness and alteration rate of the CaO/ZnO-modified waste loaded glass were significantly lower than for the non-modified counterpart, with alteration rates of  $0.9 \pm 0.1 \text{ g m}^{-2} \text{ d}^{-1}$  for MWCZ-25 and  $3.7 \pm 0.04 \text{ g m}^{-2} \text{ d}^{-1}$  for MW25, respectively; a factor of  $\sim 4.1$  lower. This is in agreement with previous studies that have shown a beneficial effect of ZnO on early dissolution kinetics [7,9,10], which is attributed to an increase in network polymerisation through the formation of Zn-O-Si linkages, as observed by Raman spectroscopy [7], XAS [8] and predicted by molecular dynamics simulations [22]. However, while the addition of ZnO has generally been shown to enhance initial durability, a number of studies report that this may increase the long-term “residual” glass dissolution rate through the formation of Zn-smectite clays [12]. Such phases were not identified in the present study, therefore, further investigation of the dissolution kinetics, from initial to residual rates, using less aggressive dissolution techniques, is required to further underpin the geological disposal of CaO/ZnO - containing UK high level waste glass.

## 5. Conclusions

The vapour phase hydration test was applied to determine the effect of CaO/ZnO modification to the UK high level waste base glass, MW, with and without 25 wt% simulant waste loading. The resulting glass coupons were analysed by SEM/EDX and XRD, to determine the rate of gel layer formation and to provide chemical information on the precipitated species formed. The addition of simulant waste oxides to both base glass compositions was shown to significantly improve the durability. Precipitated phases in the non-modified glass compositions were found to comprise a Na-Al-silicate and clay. The addition of CaO/ZnO resulted a different phase assemblage of precipitates, including hydrated Ca- and Zn-silicates. Quartz was found to precipitate in both systems. The addition of CaO/ZnO to the waste-loaded glass composition resulted in a dramatic reduction in gel layer thickness and alteration rate (by a factor of  $\sim 4.1$ ) compared to waste-loaded, non-modified glass, suggesting that such a modification may improve the overall durability.

## Acknowledgements

This work was funded by EPSRC under grant EP/F055412/1: Decommissioning Immobilisation And Management of Nuclear Wastes for Disposal (DIAMOND), and in part by EPSRC under grant EP/L014041/1: Decommissioning, Immobilisation and Storage Solutions for Nuclear Waste Inventories (DISTINCTIVE). CLC is grateful to The University of Sheffield for the award of a Vice Chancellor's Fellowship and NCH would like to thank the Royal Academy of Engineering and the Nuclear Decommissioning Authority for funding. This research was performed, in part, at the MIDAS facility, at the University of Sheffield, which was established with support from the Department of Energy and Climate Change.

## References

- [1] A. Jiricka, J.D. Vienna, P. Hrma, D.M. Strachan, *J. Non-Cryst. Solids* 292 (2001) 25.
- [2] S. Gin, A. Abdelouas, L.J. Criscenti, W.L. Ebert, K. Ferrand, T. Geisler, M.T. Harrison, Y. Inagaki, S. Mitsui, K.T. Mueller, J.C. Marra, C.G. Pantano, E.M. Pierce, J.V. Ryan, J.M. Schofield, C.I. Steefel, *J.D. Vienna, Mat. Today* 16 (2013) 243.
- [3] J.S. Luo, W.L. Ebert, J.J. Mazer, J.K. Bates, *Mat. Res. Soc. Symp. Proc.* 465 (1997) 157.
- [4] E.M. Pierce, B.P. McGrail, M.M. Valenta, D.M. Strachan, *Nucl. Technol.* 155 (2006) 149.
- [5] E. Curti, J.L. Crovisier, G. Morvan, A.M. Karpoff, *Appl. Geochem* 21 (2006) 1152.
- [6] C.L. Corkhill, N.J. Cassingham, P.G. Heath, N.C. Hyatt, *Int. J. Appl. Glass. Sci.* 4 (2013) 341.
- [7] H. Zhang, C.L. Corkhill, P.G. Heath, R.J. Hand, M.C. Stennett, N.C. Hyatt, *J. Nucl. Mater* 462 (2015) 321.
- [8] N. Cassingham, M.C. Stennett, P.A. Bingham, N.C. Hyatt, *Int. J. Appl. Glass Sci.* 2 (2011) 343.
- [9] G. Calestani, A. Monternero, E. ferraguti, G. Ingeletto, M. Bettinelli, *J. Non-Cryst. Solids* 84 (1986) 452.
- [10] G. Della Mea, A. Gaspatro, M. Bettelini, A. Montenero, R. Scaglioni, *J. Non-Cryst. Solids* 81 (1986) 443.
- [11] S. Gin, P. Frugier, P. Jollivet, F. Bruguier, *Int. J. Appl. Glass Sci.* 4 (2013) 371.
- [12] M. Fournier, S. Gin, P. Frugier, *J. Nucl. Mater* 448 (2014) 348.
- [13] Standard Test Method for Measuring Waste Glass or Glass Ceramic Durability by Vapor Hydration Test (VHT). ASTM C1663–09, American Society for Testing and Materials, Philadelphia, 2008.
- [14] N. Hyatt, W.E. Lee, R.J. Hand, P.K. Abraitis, C.R. Scales, *Mat. Res. Symp. Proc.* 807 (2004) 181.
- [15] W.L. Gong, L.M. Wang, R.C. Ewing, E. Vernaz, J.K. Bates, W.L. Ebert, *J. Nucl. Mater* 254 (1998) 249.
- [16] J. Neeway, A. Abdelouas, B. Grambow, S. Schumacher, C. Martin, M. Kogawa, S. Utsunomiya, S. Gin, P. Frugier, *J. Non-Cryst. Solids* 358 (2012) 2894.
- [17] T. Geisler, M.R. Nagel, A. Kilburn, J.P. Janssen, R.O.C. Icenhower, M. Fonseca, A.A. Grange, Nemchin, *Geochim. Cosmochim. Acta* 158 (2015) 112.
- [18] M. Harrison, C.J. Steele, A.D. Riley, *Glass Technol. Eur. J. Glass Sci. Technol. A* 53 (2012) 211.
- [19] M. Neyret, M. Lenoir, A. Grandjean, N. Massoni, B. Penelon, M. Malki, *J. Non-Cryst. Solids* 410 (2015) 74.
- [20] N. Cassingham, C.L. Corkhill, D.J. Backhouse, R.J. Hand, J.V. Ryan, J.D. Vienna, N.C. Hyatt, *Min. Mag.* 79 (2015) 1529.
- [21] J. Caurel, E. Vernaz, D. Beaufort, *Mat. Res. Soc. Proc.* 176 (1990) 309.
- [22] T. Stetchert, M.J.D. Rushton, R.W. Grimes, *J. Am. Ceram. Soc.* 96 (2013) 402.